

Statistical Characterization and Mitigation of NLOS Errors in UWB Localization Systems

Francesco Montorsi

Department of Information Engineering
University of Modena and Reggio Emilia
Modena, Italy 0039-0592056323
Email: francesco.montorsi@unimore.it

Fabrizio Pancaldi

Department of Science and
Methods for Engineering
University of Modena and Reggio Emilia
Reggio Emilia, Italy 0039-0592056323
Email: fabrizio.pancaldi@unimore.it

Giorgio M. Vitetta

Department of Information Engineering
University of Modena and Reggio Emilia
Modena, Italy 0039-0592056323
Email: giorgio.vitetta@unimore.it

Abstract—In this paper some new experimental results about the statistical characterization of the *non-line-of-sight* (NLOS) bias affecting *time-of-arrival* (TOA) estimation in *ultrawideband* (UWB) wireless localization systems are illustrated. Then, these results are exploited to assess the performance of various *maximum-likelihood* (ML) based algorithms for joint TOA localization and NLOS bias mitigation. Our numerical results evidence that the accuracy of all the considered algorithms is appreciably influenced by the LOS/NLOS conditions of the propagation environment.

Index Terms—Ultra Wide Band (UWB), Radiolocalization, Bias mitigation.

I. INTRODUCTION

Wireless localization in harsh communication environments (e.g., in a building where wireless nodes are separated by concrete walls and other obstacles) can be appreciably affected by direct path attenuation and NLOS conditions. Various solutions for NLOS error mitigation in UWB environments are available in the technical literature [1], [2], [3], [4]. A simple deterministic model, dubbed *wall extra delay*, is proposed in [1] to estimate the bias introduced by walls. A non-parametric support vector machine is employed in [2] for joint bias mitigation and channel status detection; this approach exploits multiple features extracted from received signals in a non-statistical fashion. A few classification algorithms for LOS/NLOS detection are compared in [3], where it is shown that the best solution is offered by a statistical strategy based on the joint *probability density function* (pdf) of the delay spread and the kurtosis extracted from the received signals. Finally, in [4] statistical models for the *time of arrival* (TOA), the *received signal strength* (RSS) and the *root mean square delay spread* (RDS) are developed and an iterative estimator for bias mitigation is devised.

The contribution of this paper is twofold. In fact, first of all, the problem of joint statistical modeling of multiple features extracted from a database of waveforms acquired in a TOA-based localization system is investigated. Note that, as far as we know, in the technical literature only univariate models for bias mitigation have been proposed until now (e.g., see [1], [4]). The use of multiple signal features in UWB localization systems has been investigated in [3] for channel

state detection only and in [5], where, however, the considered features (namely, the kurtosis, the mean excess delay and the delay spread) are modelled as independent random variables. The second contribution is represented by a performance comparison of various *maximum-likelihood* (ML) estimators for TOA-based localization. In particular, unlike other papers (e.g., see [2], [3]) we illustrate some numerical results referring to the accuracy of different localization strategies, rather than to the bias removal on a single radio link.

The remaining part of this paper is organized as follows. In Section II some information about our UWB experimental campaign and about the features extracted from the acquired data are provided. In Section III some estimation algorithms for UWB radiolocalization are described, whereas their performance is compared in Section IV. Finally, some conclusions are given in Section V.

II. EXPERIMENTAL SETUP

A. Measurement arrangement

A measurement campaign has been conducted by our research group in 2010; it is worth mentioning that various databases providing a collection of sampled UWB waveforms acquired in experimental campaigns and useful for assessing the performance of localization algorithms are already available (e.g., see [6], [7]). However, our database has been specifically generated to assess the correlation between the NLOS bias error and various features extracted from the received signals, as it will become clearer in the next Paragraph.

All the measured data were acquired by means of two FCC-compliant PulsON220 radios commercialised by TimeDomain and were collected in a database. Such devices are equipped with omnidirectional antennas, are characterized by a -10 dB bandwidth and a central frequency equal to 3.2 GHz and 4.7 GHz, respectively, and perform two-way TOA ranging; they also allow to store the digitised received waveforms (a sampling frequency of 24.2 GHz and 14 bits per sample are used). Our measurement campaign consisted of two phases. First, the transmitter was placed in a given room (room A in Fig. 1) and the receiver in an adjacent room (room B in Fig. 1) separated from the room A by a wall having thickness $t_{wall} = 32$ cm (NLOS condition); in addition, the transmit

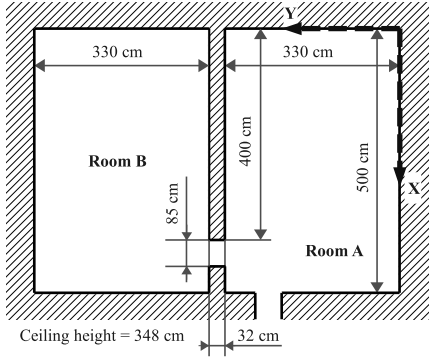


Figure 1. Map of the environment of our experimental campaign.

antenna was kept fixed, whereas the receive antenna was placed in $N_{acq}^{NLOS} = 174$ distinct vertices of a dense square grid (the distance between a couple of nearest vertices was equal to 21 cm). In the second phase of our measurement campaign the transmitter and receiver were both placed in room B (LOS condition); then, the transmit antenna was kept fixed, whereas the receive antenna was moved on the same dense grid as in the first phase, to acquire the UWB signal in $N_{acq}^{LOS} = 105$ distinct vertices. The distance between the two antennas varied between 1 m and about 5 m; larger distances were not taken into consideration since we were interested in indoor ranging only. It is important to note that the choice of the measurement scenarios described above is motivated by the fact that the UWB signals experienced similar propagation in both phases.

For each grid position, besides the acquired waveform, a TOA estimate (evaluated by the PulsON220 devices) and the actual transmitter-receiver distance (evaluated by means of a metric tape with an accuracy better than 1 cm) were also stored in the database. The TOA estimates have been used to provide a common time frame to all the acquired waveforms; this has made possible the estimation of the mean excess delay and of other signal statistics in the signal processing phase.

B. Statistical modeling of signal features

The model

$$\tau_i = \frac{d_i}{c_0} + b_i + w_i \quad (1)$$

was adopted for the i -th link for both LOS and NLOS conditions. Here, τ_i denotes the TOA estimated by the PulsON220 devices, based on energy thresholds and a go-back technique (see [8] for further details), c_0 is the speed of light, d_i denotes the distance between the transmitter and the receiver, b_i is the NLOS bias (in seconds) affecting the TOA measurement (the values taken on by this random parameter are always positive for NLOS links and null for LOS links¹) and $w_i \sim \mathcal{N}(0, \sigma_{w,i}^2)$ is the measurement noise; in addition, the expression $\sigma_{w,i}^2 = \gamma \sigma_n^2 d_i^\beta$ is adopted for the variance of the measurement noise, where γ is a parameter depending on both the specific TOA estimator employed in the ranging

¹In this case the probability density function (pdf) of b_i is $f_b(b) = \delta(b)$.

Correlation with b_i	$x_{i,0}$	$x_{i,1}$	$x_{i,2}$	$x_{i,3}$	$x_{i,4}$	$x_{i,5}$	d_i
NLOS case	0.795	0.852	0.894	0.641	0.454	0.644	0.609
LOS case	0.602	0.586	0.129	0.666	0.586	0.119	0.629

Table I
ABSOLUTE VALUE OF THE CORRELATION COEFFICIENT BETWEEN b_i AND EACH FEATURE OF THE SET $\{x_{i,j}, j = 0, 1, \dots, 5\}$.

measurements and on various parameters of the physical layer, and β is the path-loss exponent (a known and fixed value is assumed for this parameter in both LOS and NLOS conditions [4]).

In the following we focus on the problem of estimating the bias b_i (affecting the TOA estimate τ_i (1)) from a set of $N_f = 6$ different “features” $\{x_{i,j}, j = 0, 1, \dots, 5\}$ extracted from the received waveform $r_i(t)$. In particular, like in [2], the following features have been evaluated for the set of the received waveforms:

- 1) the maximum signal amplitude $x_{i,0} = r_{max,i} \triangleq \max_t |r_i(t)|$;
- 2) the mean excess delay $x_{i,1} = \tau_{m,i} \triangleq \int_0^\infty t \frac{|r_i(t)|^2}{\varepsilon_i} dt$ (the parameter ε_i is defined below);
- 3) the delay spread $x_{i,2} = \tau_{ds,i} \triangleq \int_0^\infty (t - \tau_{m,i})^2 \frac{|r_i(t)|^2}{\varepsilon_i} dt$;
- 4) the energy $x_{i,3} = \varepsilon_i \triangleq \int_0^\infty |r_i(t)|^2 dt$;
- 5) the rise time $x_{i,4} = t_{rise,i} \triangleq \min \{t : |r_i(t)| / \max_t |r_i(t)| > 0.9\} - \min \{t : |r_i(t)| / \max_t |r_i(t)| > 0.1\}$;
- 6) the kurtosis $x_{i,5} = \kappa_i \triangleq \frac{1}{\sigma_{|r|}^4 T} \int_T (|r_i(t)| - \mu_{|r|})^4 dt$, where $\mu_{|r|} \triangleq \frac{1}{T} \int_T |r_i(t)| dt$, $\sigma_{|r|}^2 \triangleq \frac{1}{T} \int_T (|r_i(t)| - \mu_{|r|})^2 dt$ and T denotes the observation time.

In the following the set $\{r_i(t)\}$ of received waveforms is modelled as a random process, so that the above mentioned features form a set of correlated random variables; in addition, all of them are statistically correlated with the TOA bias. The last consideration is confirmed by the numerical results of Table I, which lists the absolute values of the correlation coefficients of the previously described features with the estimated TOA bias for both the LOS and the NLOS scenarios. From these results it can be easily inferred that not all the considered features are equally useful to estimate the TOA bias. For this reason and to simplify our statistical analysis, we restricted the set of features to $\{x_{i,0}, x_{i,1}, x_{i,2}\}$ ($N_f = 3$), which collects the parameters exhibiting a strong correlation with the bias in the NLOS scenario.

Note that, in principle, the bias b_i is not influenced by the distance d_i , since it depends only on the thickness of the walls (or of other obstacles) encountered by the transmitted signal during its propagation; this is not true, however, for the above mentioned triple of signal features (see [1] for further details). Generally speaking, it is useful to derive a TOA bias estimator which is not influenced by the transmitter-receiver distance d_i . Therefore, in the attempt of removing the dependence of the features $\{x_{i,0}, x_{i,1}, x_{i,2}\}$ on the link distance, we developed the models $x_{i,0} = r_{max,i} = r_{max}^0 - r_{max}^m d_i$,

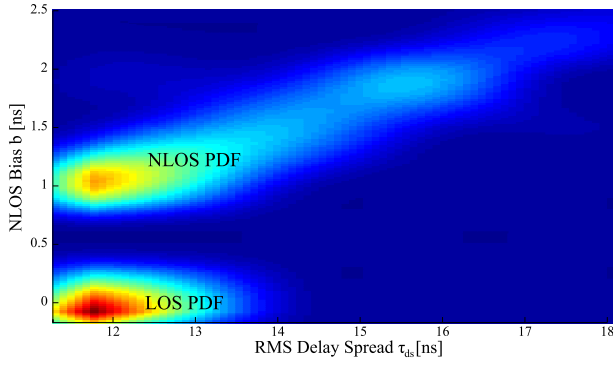


Figure 2. Estimated joint pdf of the estimated TOA bias and the delay spread in NLOS conditions (above) and LOS conditions (below).

$x_{i,1} = \tau_{m,i} = \tau_m^m d_i$ and $x_{i,2} = \tau_{ds,i} = \tau_{ds}^0 + \tau_{ds}^m d_i$ on the basis of our experimental results and, in particular, on the basis of the estimates of the joint pdf's $\{f_{b,x_0}, f_{b,x_1}, f_{b,x_2}\}$ referring to the three possible couples $(b_i, x_{i,j})$ with $j = 0, 1, 2$ and $i = 0, 1, \dots, N_{acq} - 1$, where $N_{acq} = N_{acq}^{NLOS} + N_{acq}^{LOS}$; here r_{max}^0 , τ_m^m and τ_{ds}^m are random variables, whereas τ_{ds}^0 and r_{max}^m are deterministic parameters having known values (all are assumed independent of d_i and thus also from the link index i). Given these models, the vector of distance-independent features $\tilde{\mathbf{x}} \triangleq [r_{max}^0, \tau_m^m, \tau_{ds}^m]^T$ can be evaluated from its distance-dependent counterpart² $\mathbf{x} = [r_{max}, \tau_m, \tau_{ds}]^T$ and can be used in place of it. However it turns out that parameters of $\tilde{\mathbf{x}}$ are less correlated with b_i than those of \mathbf{x} ; for this reason, we decided to take into consideration both for localization purposes (see Sec. III-B2).

A complete statistical characterization of the estimated bias and of the 3 related signal features we consider is provided by the joint pdf $f_{b,r_{max},\tau_m,\tau_{ds}}(\cdot)$ or, equivalently, by the joint pdf $f_{b,r_{max}^0,\tau_m^m,\tau_{ds}^m}(\cdot)$ (both can be estimated from the acquired data). Some marginalizations, like the one shown in Fig. 2, reveal interesting aspects: 1) a significant (limited) correlation between these parameters is found in the NLOS (LOS) case; 2) the null region exhibited by the estimated pdf's is due to the fact that the TOA bias cannot take on values in the interval $[0, t_{wall}/c_0]$, where t_{wall} is the thickness of the wall obstructing the direct path; 3) large values of the TOA bias are unlikely since they are associated with small incidence angles of the transmitted signal on the obstructing wall.

III. LOCALIZATION ALGORITHMS

A. Introduction

In this Section we develop various algorithms for two-dimensional localization in a UWB network composed by N_a anchors with *known* positions $\mathbf{z}_i^a \triangleq [x_i^a, y_i^a]^T \in \mathbb{R}^2$, $i = 0, \dots, N_a - 1$ and by a single node (dubbed mobile station, MS, in the following) with *unknown* position $\boldsymbol{\theta} \triangleq [x, y]^T \in \mathbb{R}^2$. Any couple of the given $(N_a + 1)$ devices can operate in a LOS (NLOS) condition with probability P_{LOS}

²In the rest of the document, the subscript i has been omitted for simplicity when not strictly necessary.

$(1 - P_{LOS})$. The localization algorithms described below try to mitigate the effects of the NLOS bias error and aim at generating an estimate $\hat{\boldsymbol{\theta}}$ of $\boldsymbol{\theta}$ minimizing the *mean square error* (MSE) $\mathbb{E}_{\hat{\boldsymbol{\theta}}} \left\{ \|\hat{\boldsymbol{\theta}} - \boldsymbol{\theta}\|^2 \right\}$. It is also important to point out that localization algorithms developed for NLOS scenarios usually consist of two steps. In fact, first the NLOS bias is estimated for each involved link and is used to remove the bias contribution in the acquired data; then the new data set is processed by a *least-square* (LS) procedure generating an estimate of $\boldsymbol{\theta}$ (e.g., see [2], [3], [4], [5]). In the following instead, implicit estimation of the bias for each link is adopted; this approach is motivated by the fact that the estimation of the bias for the i -th link can benefit from the information acquired from the other $(N_a - 1)$ links; note that in [2] and [5] bias mitigation performed in a link-by-link fashion is exploited to assign a weight in a *weighted least-square* (WLS) step but such an approach is heuristic and differs from our ML-based approach.

B. Maximum Likelihood Estimation

If the links between the MS and the N_a different anchors are assumed mutually independent, the ML estimation strategy of the unknown MS position $\boldsymbol{\theta}$, given a TOA estimate and a set of additional signal features for each link, can be formulated as $\hat{\boldsymbol{\theta}} = \arg \max_{\tilde{\boldsymbol{\theta}}} \ln \prod_{i=0}^{N_a-1} f_{\tau,\mathbf{x}}(\tau_i, \mathbf{x}_i; \tilde{\boldsymbol{\theta}})$, where $\tilde{\boldsymbol{\theta}} = [\tilde{x}, \tilde{y}]^T \in \mathbb{R}^2$ denotes the MS trial position, τ_i and \mathbf{x}_i are the TOA and N_f -dimensional signal vector collecting the received signal features acquired for the i -th link and $f_{\tau,\mathbf{x}}(\cdot, \cdot; \tilde{\boldsymbol{\theta}})$ is the joint pdf of the TOA and the vector of features parameterized by the trial position $\tilde{\boldsymbol{\theta}}$. In the following Paragraphs the impact of various possible options for the ML strategy are investigated.

1) *ML estimation strategy for different sets of observed data*: in this Paragraph two different options are considered for the set of features processed by the ML strategy.

a) *Option A*: in this case it is assumed that the vector of features referring to the i -th link is $\mathbf{x}_i = [r_{max,i}, \tau_{m,i}, \tau_{ds,i}]^T$; this choice is motivated by the large correlation between these random variables and the link bias b (see Paragraph II-B). Then, the joint PDF $f_{\tau,\mathbf{x}}(\tau_i, \mathbf{x}_i; \tilde{\boldsymbol{\theta}})$ appearing in the ML strategy can be expressed as (see Eq. (1)):

$$f_{\tau,\mathbf{x}}(\tau_i, \mathbf{x}_i; \tilde{\boldsymbol{\theta}}) = (f_{b,\tilde{\mathbf{x}}} \otimes f_w) \left(\tau_i - \frac{d_i(\tilde{\boldsymbol{\theta}})}{c_0}, \tilde{\mathbf{x}}_i \right), \quad (2)$$

where

$$\tilde{\mathbf{x}}_i = \left[r_{max,i} + r_{max}^m d_i(\tilde{\boldsymbol{\theta}}), \frac{\tau_{m,i}}{d_i(\tilde{\boldsymbol{\theta}})}, \frac{\tau_{ds,i} - \tau_{ds}^0}{d_i(\tilde{\boldsymbol{\theta}})} \right]^T \quad (3)$$

(because of the models previously described for r_{max}^0 , τ_m^m and τ_{ds}^m), $d_i(\tilde{\boldsymbol{\theta}})$ is the distance between the i -th anchor and the MS trial position and $f_{b,\tilde{\mathbf{x}}} \otimes f_w$ denotes the convolution between the joint pdf $f_{b,\tilde{\mathbf{x}}}(\cdot)$ and the observation noise pdf $f_w(w) = (2\pi\sigma_w^2)^{-1/2} \exp(-w^2/(2\sigma_w^2))$.

Note that the shape of the function $f_{b,\tilde{\mathbf{x}}}(\cdot)$ under the *hypothesis of LOS conditions* (H_{LOS} event) is substantially different

from that found in NLOS conditions (H_{NLOS} event) [4]; for this reason, we estimated this function in both cases applying the procedure described in [1] to the data collected in our measurement campaign; this led to two distinct multidimensional histograms, which approximate the pdf's $f_{b,\tilde{\mathbf{x}}}(b, \tilde{\mathbf{x}}_i | H_{\text{LOS}})$ and $f_{b,\tilde{\mathbf{x}}}(b, \tilde{\mathbf{x}}_i | H_{\text{NLOS}})$ with a certain accuracy depending on: a) the quantity of acquired data; b) the sizes Δb , Δr_{max} , $\Delta \tau_m$ and $\Delta \tau_{ds}$ of the quantization bins adopted in the generation of the histograms. Note that these sizes need to be accurately selected, since large bins imply a coarse approximation of pdf's, whereas excessively small bins require a huge amount of data.

Given an estimate of the above mentioned couple of pdf's, the required pdf $f_{b,\tilde{\mathbf{x}}}(\cdot)$ can be trivially evaluated using the law of total probability and the $P_{\text{LOS}} \triangleq \Pr\{H_{\text{LOS}}\}$ and $P_{\text{NLOS}} \triangleq \Pr\{H_{\text{NLOS}}\} = 1 - \Pr\{H_{\text{LOS}}\}$ probabilities when they are available, or assuming $P_{\text{LOS}} = P_{\text{NLOS}} = 0.5$ if no *a priori* information about the LOS/NLOS conditions are available.

b) *Option B*: in this case the set of features employed in ML estimation consists of a single element, namely the delay spread (which exhibits the largest correlation with the NLOS bias; see Table I), so that $\mathbf{x}_i = \tau_{ds,i}$ and the pdf $f_{\tau,\mathbf{x}}(\tau_i, \mathbf{x}_i; \tilde{\boldsymbol{\theta}})$ of the ML strategy becomes (see (2))

$$f_{\tau,\mathbf{x}}(\tau_i, \mathbf{x}_i; \tilde{\boldsymbol{\theta}}) = (f_{b,\tau_{ds}^m} \otimes f_w) \left(\tau_i - \frac{d_i(\tilde{\boldsymbol{\theta}})}{c_0}, \frac{\tau_{ds,i} - \tau_{ds}^0}{d_i(\tilde{\boldsymbol{\theta}})} \right) \quad (4)$$

Like in the previous case, the pdf $f_{b,\tau_{ds}^m}(\cdot)$ has to be estimated in the LOS and NLOS scenarios (see Fig. 2) from the data acquired in our measurement campaign. Note that this option leads to a ML localization algorithm which is substantially simpler than that proposed in the analysis of option A.

2) *Parameterization of the observations*: the ML strategies developed above are based on the joint pdf's $f_{b,r_{max}^0, \tau_m^m, \tau_{ds}^m}(\cdot)$ and $f_{b,\tau_{ds}^m}(\cdot)$ which refer to a set of *distance-independent parameters*. Since the parameters r_{max}^0 , τ_m^m and τ_{ds}^m exhibit a lower correlation with b than their distance-dependent counterparts r_{max} , τ_m , τ_{ds} , we believe that the use of the joint PDF

$$f_{\tau,\mathbf{x}}(\tau_i, \mathbf{x}_i; \tilde{\boldsymbol{\theta}}) = (f_{b,\mathbf{x}} \otimes f_w) \left(\tau_i - \frac{d_i(\tilde{\boldsymbol{\theta}})}{c_0}, \mathbf{x}_i \right) \quad (5)$$

in place of (2) deserves to be investigated (similar comments hold for (4)).

3) *Estimation of joint pdf's*: as already explained above, the joint pdf's involved in the proposed ML localization strategies can be easily estimated from the acquired data using a simple procedure based on dividing the space of observed data in a set of bins of proper size. Such a procedure generates an histogram, which, unluckily, entails poor localization performance if employed as it is, because of the relatively small number of bins (adopted to avoid empty bins). To mitigate this problem either interpolation followed by low-pass filtering can be applied to raw experimental histograms (this leads to *interpolated-histogram estimators*) or the raw data can be

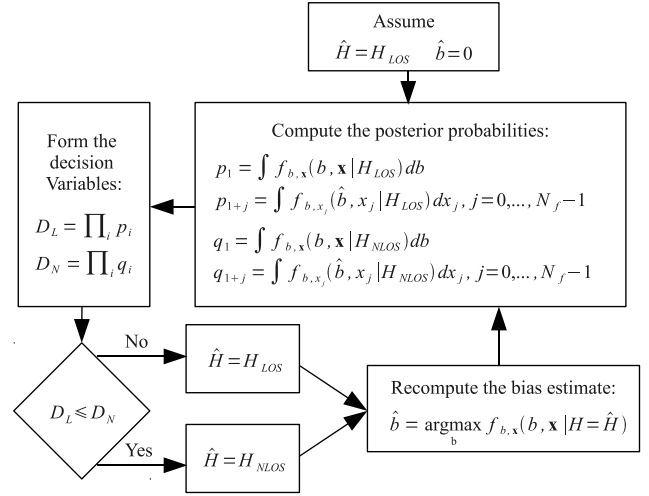


Figure 3. Flow diagram of the proposed iterative estimator.

fitted with analytical functions (this results in *fitted-histogram estimators*).

C. Iterative Estimation

Recently, an iterative estimator of both the channel state (i.e., LOS or NLOS conditions) and the NLOS bias b has been proposed in [4]. In Fig. 3 the flow diagram of a modified version of this iterative algorithm, employing the joint pdf's described above and extracted from our experimental database, is proposed. Note that this algorithm operates in a link-by-link fashion (in the diagram of Fig. 3 the link index i has been omitted to ease the reading).

IV. NUMERICAL RESULTS

Our experimental database has also been exploited to assess the RMSE performance of the proposed algorithms for localization and NLOS bias mitigation schemes via computer simulations. In our simulations the MS coordinates are always $(0; 0)$; then, following [2], for the i -th anchor a received waveform from either the LOS database (with probability P_{LOS}) or from the NLOS database (with probability P_{NLOS}) was drawn randomly and was associated with the position $\mathbf{z}_i^a = \left(d_i \sin(2\pi \frac{i-1}{N_a}); d_i \cos(2\pi \frac{i-1}{N_a}) \right)$, where d_i is the distance measured for the selected waveform. Note that these waveforms already include the experimental noise and thus no simulated noise was imposed on the waveforms (so that the signal-to-noise ratio is the experimental one). Finally, the parameter N_a has been set to 3 (worst case which still theoretically allows unambiguous localization).

The RMSE performance of the following algorithms has been evaluated:

- 1) **LS** - A standard LS estimator for LOS environments; the estimation strategy can be expressed as $\hat{\boldsymbol{\theta}} = \arg \min_{\boldsymbol{\theta}} \sum_{i=0}^{N_a-1} (c_0 \tau_i - d_i(\boldsymbol{\theta}))^2$.
- 2) **VE** - A LS estimator exploiting TOA measurements corrected by the algorithm proposed by Venkatesh and Buehrer in [4]; this algorithm relies on a statistical

modeling of the propagation environment based on our experimental database.

- 3) **ML-4D** - A ML estimator based on (2) and employing an interpolated histogram, in the likelihood function, referring to a distance-dependent parameterization.
- 4) **ML-2D** - A ML estimator based on (4) and employing an interpolated histogram, in the likelihood function, referring to a distance-dependent parameterization.
- 5) **ML-2D-ID** - A ML estimator based on (4) and employing an interpolated, histogram in the likelihood function, referring to a distance-independent parameterization.
- 6) **ML-4D-F** - A ML estimator based on (2) and employing a *fitted* histogram, in the likelihood function, referring to a distance-dependent parameterization.
- 7) **ML-4D-IT** - A LS estimator based on (2) and exploiting TOA measurements corrected by the modified *iterative* algorithm illustrated in Section III-C.
- 8) **ML-2D-IT** - A LS estimator based on (4) and exploiting TOA measurements corrected by the modified *iterative* algorithm illustrated in Section III-C.

In estimating the RMSE performance of the ML algorithms listed above the likelihood functions were always evaluated at the vertices of a square grid characterized by a step size equal to 10 mm. Some numerical results are compared in Fig. 4, which illustrates the RMSE performance versus the probability P_{LOS} . These results evidence that:

- 1) The simple LS algorithm is outperformed by all the other algorithms when $P_{\text{LOS}} \leq 0.9$; this is due to the fact that this strategy does not try to mitigate NLOS bias.
- 2) The VE algorithm performs well at the cost of a reasonable complexity, but offers limited bias mitigation when $P_{\text{LOS}} = 0$; in this case the ML-2D, ML-2D-ID and ML-4D-F estimators perform much better.
- 3) The exploitation of a large set of received signal features does not necessarily allow to achieve better accuracy than a subset of them (see the curves referring to ML-2D and ML-4D estimators); this is due to the fact that the correlation between the different couples of extracted features is typically large, so that they provide strongly correlated information about the NLOS bias.
- 4) Distance-dependent parameterization provides better accuracy (see the curves referring to the ML-2D and ML-2D-ID estimators); this can be related to the fact that τ_{ds}^m is less correlated with the NLOS bias than its distance-dependent counterpart τ_{ds} .
- 5) The ML-4D-F estimator performs better than the ML-4D estimator in NLOS conditions; this means that the use of fitted histograms entails an improvement of localization accuracy.

V. CONCLUSIONS

In this paper various UWB localization techniques processing multiple features extracted from the received signal to mitigate the problem of NLOS bias have been described and their accuracy has been assessed exploiting the experimental data

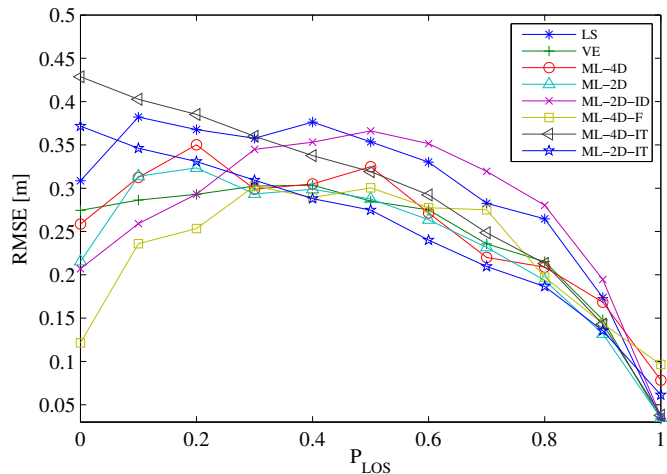


Figure 4. RMSE performance versus P_{LOS} offered by various localization algorithms.

acquired in an measurement campaign. Our results evidence that: a) a restricted set of features has to be employed; b) the use of distance-dependent features and of fitted histograms provides better performance than that offered by distance-independent features and interpolated histograms.

ACKNOWLEDGEMENTS

The authors would like to thank Prof. Marco Chiani and Prof. Davide Dardari (both from the University of Bologna, Italy) for lending us the UWB devices employed in our measurement campaign and the PhD students Alessandro Barbieri and Fabio Gianaroli for their invaluable help in our experimental work. Finally, the authors wish to acknowledge the activity of the Network of Excellence in Wireless Communications (NEWCOM++, contract n. 216715), supported by the European Commission which motivated this work.

REFERENCES

- [1] D. Dardari, A. Conti, J. Lien, and M. Z. Win, "The effect of cooperation on localization systems using UWB experimental data," *EURASIP J. Adv. Signal Process.*, vol. 2008, Jan. 2008.
- [2] S. Maranó, W. Gifford, H. Wymeersch, and M. Z. Win, "NLOS identification and mitigation for localization based on UWB experimental data," *IEEE J. Sel. Areas Commun.*, vol. 28, pp. 1026–1035, Sept. 2010.
- [3] N. Decarli, D. Dardari, S. Gezici, and A. A. D'Amico, "LOS/NLOS detection for UWB signals: A comparative study using experimental data," in *Proc. of the 5th IEEE International Symposium on Wireless Pervasive Computing (ISWPC 2010)*, pp. 169–173, May 2010.
- [4] S. Venkatesh and R. Buehrer, "Non-line-of-sight identification in ultrawideband systems based on received signal statistics," *IET Microwaves, Antennas Propagation*, vol. 1, pp. 1120–1130, Dec. 2007.
- [5] I. Güvenç, C.-C. Chong, F. Watanabe, and H. Inamura, "NLOS identification and weighted least-squares localization for UWB systems using multipath channel statistics," *EURASIP J. Adv. Signal Process.*, vol. 2008, Jan. 2008.
- [6] "WPR.B database." Available online at <http://www.vicewicom.eu>.
- [7] J.-Y. Lee, "USC ranging test database." Available online at http://ultra.usc.edu/uwb_database/ranging_test.htm.
- [8] D. Dardari, C.-C. Chong, and M. Z. Win, "Threshold-based time-of-arrival estimators in UWB dense multipath channels," *IEEE Trans. Commun.*, vol. 56, pp. 1366–1378, Aug. 2008.